

Electronic Supplementary Information (ESI)

**Regulating catalytic behaviour of Iron oxyhydroxide by introducing Ni sites for facilitating polysulfides anchoring and conversion**

Jingshuai Xiao,<sup>a</sup> Haocong Wei,<sup>a</sup> Xiao Sun,<sup>a</sup> Tengfei Yang,<sup>a</sup> Xiang Wu,<sup>a</sup> Yan Song,<sup>\*a</sup> and Chaozheng He<sup>\*a</sup>

<sup>a</sup> Institute of Environment and Energy Catalysis, Shaanxi Key Laboratory of Optoelectronic Functional Materials and Devices, School of Materials Science and Chemical Engineering, Xi'an Technological University, Xi'an, 710021, China.

\*corresponding authors: E-mail: songyan@xatu.edu.cn, hecz2019@xatu.edu.cn

## Experimental

### Synthesis of FeOOH and FeNiOOH

To synthesize  $\beta$ -FeOOH,  $\text{Fe}(\text{NO}_3)_3 \cdot 9\text{H}_2\text{O}$  (2.43 g) and  $\text{NaNO}_3$  (5.10 g) were dissolved in a solution containing a 1:5 volume ratio of ethanol to distilled water. To create a homogeneous solution, 1M hydrochloric acid was added to the mixture under vigorous stirring before transferring it to a 50 mL Teflon-lined stainless steel autoclave. This solution was kept at 120 °C for 2 hours before being cooled down to ambient temperature. Finally,  $\beta$ -FeOOH was obtained, washed twice with DI water and ethanol, and dried at 80 °C for 12 hours. For preparation of  $\beta$ -FeNiOOH, the same method as that used for  $\beta$ -FeOOH was conducted, except for adding  $\text{Ni}(\text{NO}_3)_2 \cdot 6\text{H}_2\text{O}$  (0.436 g).

### Materials characterization

The phase identification of  $\beta$ -FeOOH and FeNiOOH was performed on an X-ray powder diffraction system (Bruker D2). X-ray photoelectron spectroscopy (XPS, an ESCALAB 250Xi spectrometer) was used to investigate the element valence and composition. The surface morphology of the electrode was characterized by scanning electron microscope (SEM, JSM-7610F). To explore the adsorption of polysulfides, we analysed the samples using a Shimadzu UV-2550 and ultraviolet absorption spectroscopy. The specific surface areas and pore volumes of all samples were measured by the Brunauer-Emmett-Teller (BET) method using nitrogen adsorption and desorption isotherms on a Micromeritics (JW-BK122-B, JWGB SCI. & Tech.).

### Density functional theory calculations:

In this paper, electronic structure and structure optimisation are demonstrated using Hubbard parameter corrections (GGA + U) and the Birkenau Enzelhoff method (PBE), geometrical optimisation is carried out using the Cambridge Series of Total Energy Packages (CASTEP) code, and phonon spectral calculations are carried out on the basis

of the optimisation. A cut-off energy of 340 eV for the hypercomplex pseudopotential is considered. An energy accuracy of  $10^{-6}$  eV is employed using the ion relaxation problem. For all calculations, the Brillouin zone integrals are approximated by sums over specific k-points using the  $2 \times 2 \times 1$  superunit structure method, with a convergence accuracy of 0.01 eV/Å for the forces.

The adsorption energy ( $E_{ads}$ ) is calculated as follows:

$$E_{ads} = E_{tot} - E_{sub} - E_{sul}$$

where  $E_{tot}$  denotes the total energy of the system for the adsorption of sulphide on the substrate, and  $E_{sub}$  and  $E_{sul}$  denote the energy of the substrate and sulphide in the free state, respectively. The positive and negative values of the adsorption energy  $E_{ads}$  indicate the adsorption and exothermic values of the process. If the result is positive, it means that energy absorption is required for sulphide adsorption, i.e., the reaction process must provide some energy, and negative values mean that the sulphide is exothermic and spontaneous in the adsorption process, and the reaction proceeds easily.

The change in Gibbs free energy ( $\Delta G$ ) for each reaction step is calculated as follows:

$$\Delta G = \Delta E + \Delta ZPE - T\Delta S$$

$\Delta G$  is the free energy change and  $\Delta E$  is the total energy change directly from the DFT. In the calculation,  $\Delta ZPE$  is the change in vibrational energy at the zero point,  $T$  is the temperature, and  $\Delta S$  is the change in entropy.  $\Delta ZPE$  is calculated from the phonon spectrum, and the energy and entropy changes of the products and reactants at 298.15 K are derived directly from the geometry optimisation.

### **Battery assembly and electrochemical measurements**

Sulfur electrodes were prepared by mixing sulfur powder with catalyst at a weight ratio of 8:2. Subsequently, the 80 wt% compound and 10 wt% of conductive agents

were mixed, followed by the addition of a solution of 10 wt% of polyvinylidene fluoride (PVDF) dissolved in N-methyl-2-pyrrolidone (NMP) and continued grinding to form a homogeneous slurry. When the resulting black paste was formed, it was evenly coated on the aluminium foil using an automatic coating machine. The coated foil was then dried in a vacuum oven and cut into pole pieces with a diameter of 12 mm for use as cathode material.

The battery assembly is conducted within an inert gas-filled glove box. The assembly sequence involves assembling the positive electrode shell, positive electrode piece (previously mentioned as the prepared pole piece with a diameter of 12 mm), electrolyte, Celgard 2400 separator, electrolyte, gasket, funnel-shaped spring sheet, lithium metal sheet negative electrode, and negative battery case. The active material loading capacity is approximately 3.5 mg/cm<sup>2</sup>. The battery assembly remained in a constant temperature chamber for three hours before electrochemical performance testing. All tests underwent completion under ambient temperature conditions.

Galvanostatic charge and discharge tests were conducted using a Neware battery tester within the voltage range of 1.7 to 2.8 V. Specific capacity values were calculated based on the mass of active sulphur. All electrochemical tests were performed at room temperature. Cyclic voltammetry (CV) was conducted on an electrochemical workstation (CHI 660E) at a scanning rate of 0.1 mV s<sup>-1</sup> between 1.7 and 2.8 V versus Li/Li<sup>+</sup>. Electrochemical impedance spectroscopy (EIS) was performed using the same instrument, with a 5 mV amplitude over a frequency range of 100 kHz to 0.01 Hz.

## Supplementary Figures

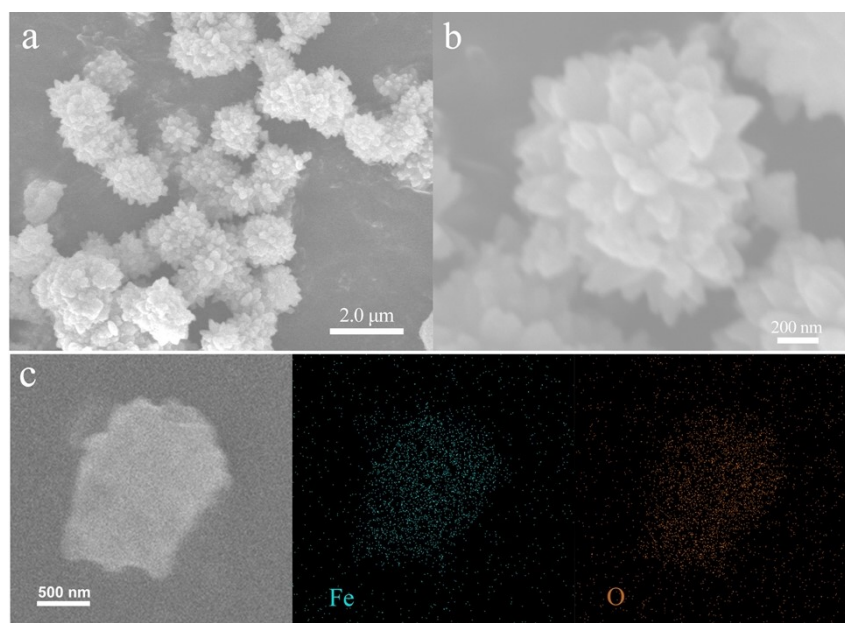


Fig. S1 (a,b) SEM images of FeOOH, (c) corresponding EDS mapping of FeOOH.

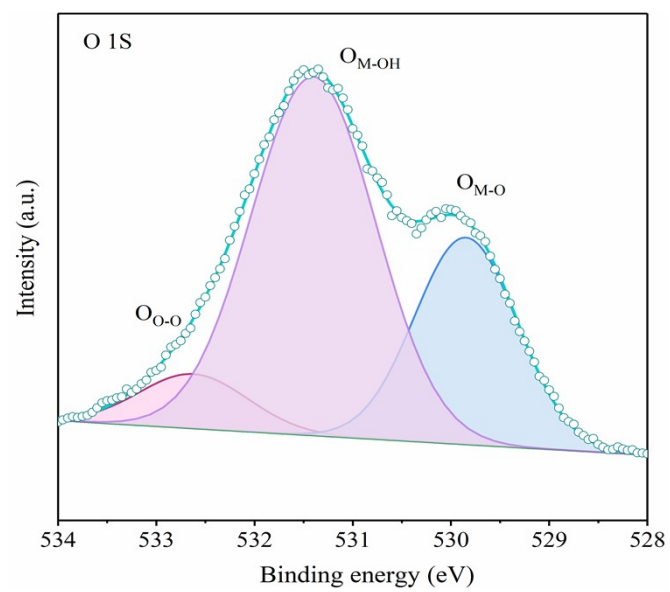


Fig. S2 O1s core-level XPS spectra of FeNiOOH.

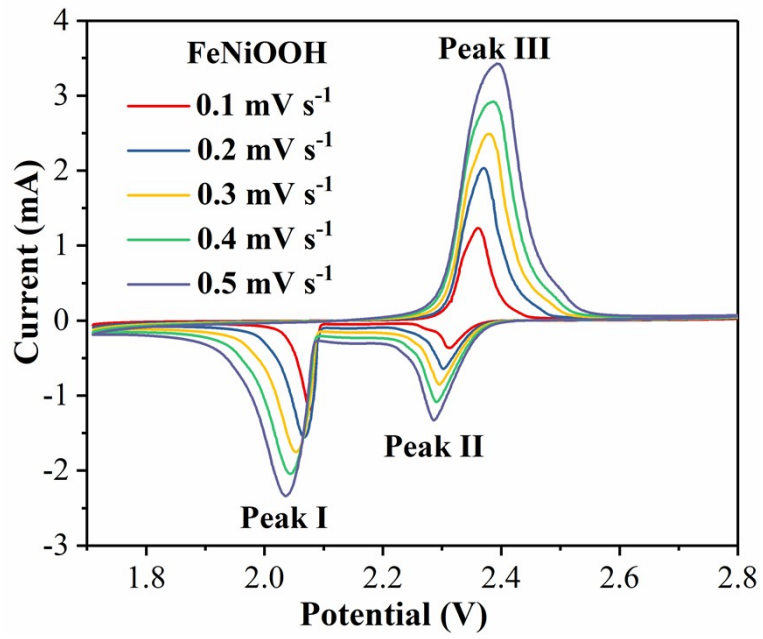


Fig. S3 CV curves of the FeNiOOH/S electrode.

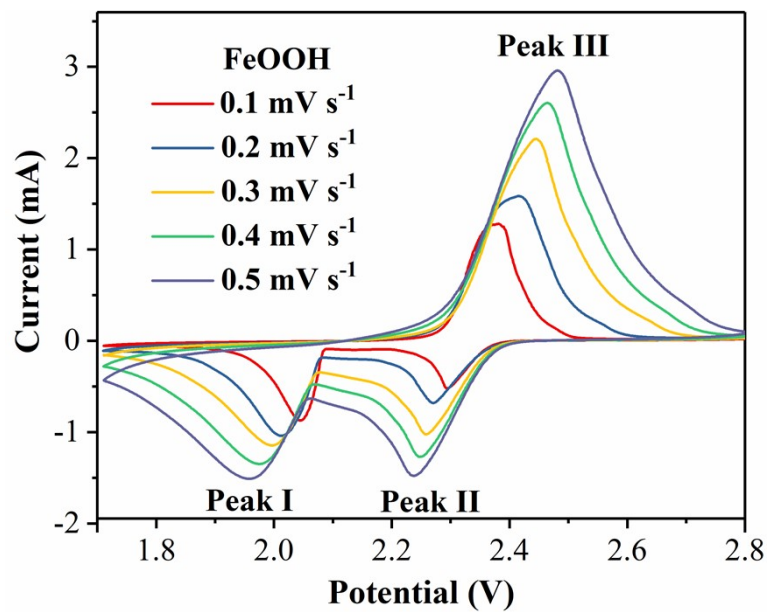


Fig. S4 CV curves of the FeOOH/S electrode.

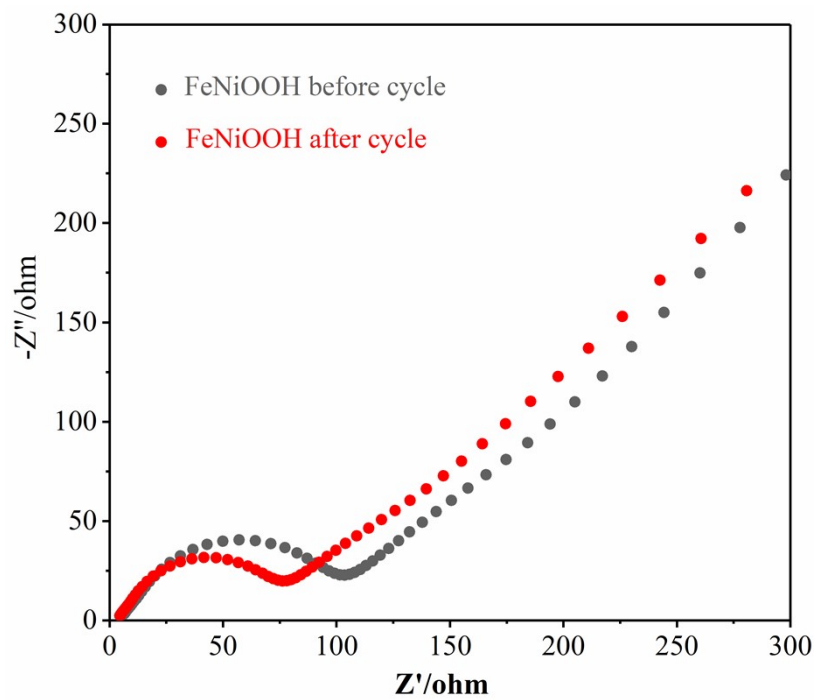


Fig. S5 Nyquist plots of the batteries with FeNiOOH before and after cycling.

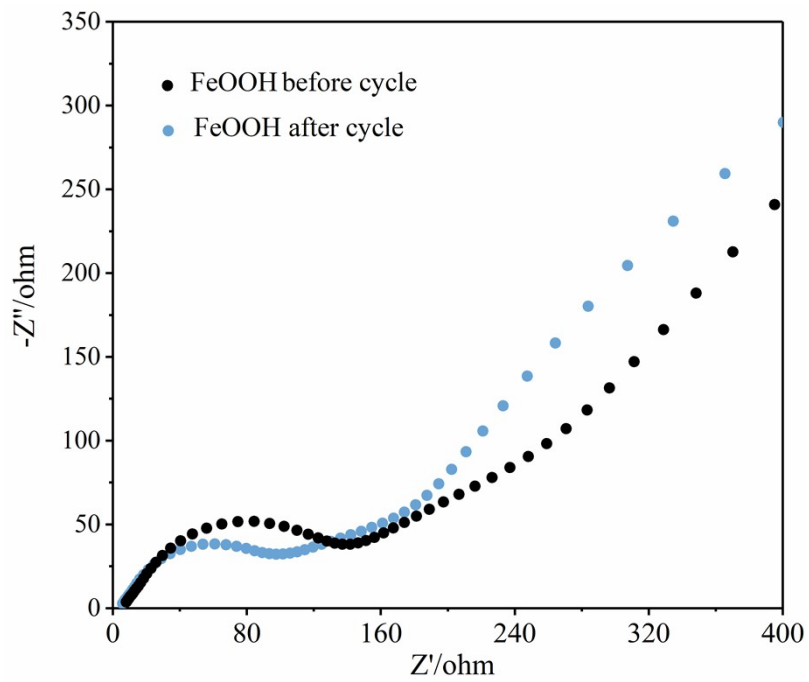


Fig. S6 Nyquist plots of the batteries with FeOOH before and after cycling.

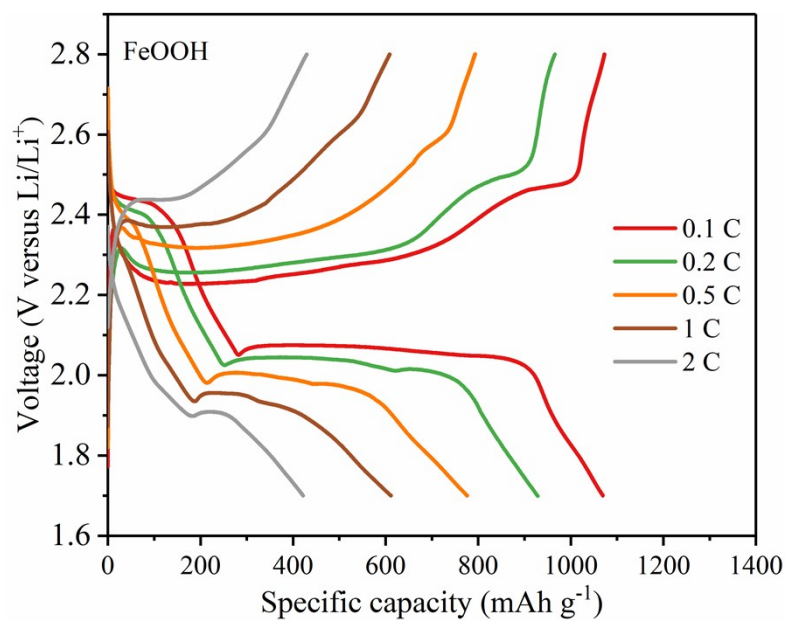


Fig. S7 Galvanostatic discharge/charge profiles of the batteries with FeOOH at current density varying from 0.1 to 2 C.

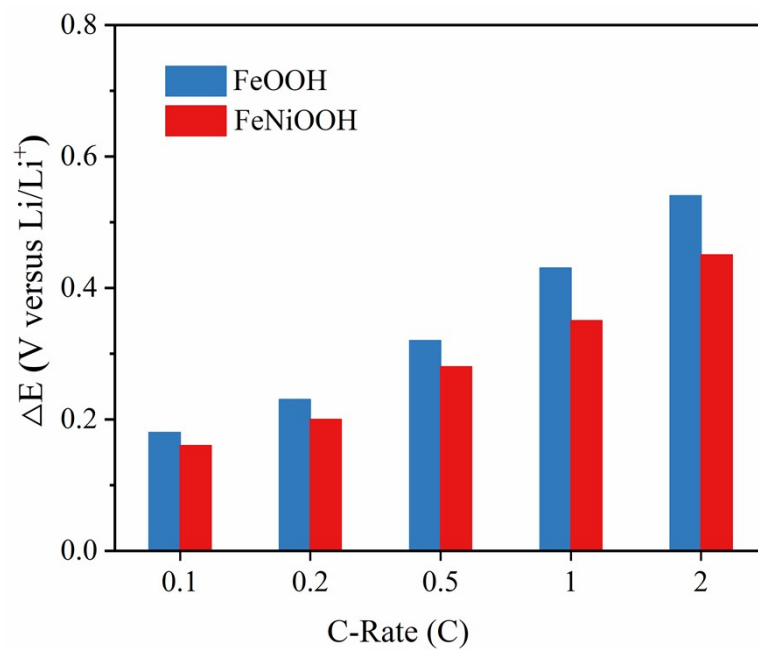


Fig. S8 Polarisation histograms of the batteries with FeNiOOH and FeOOH.

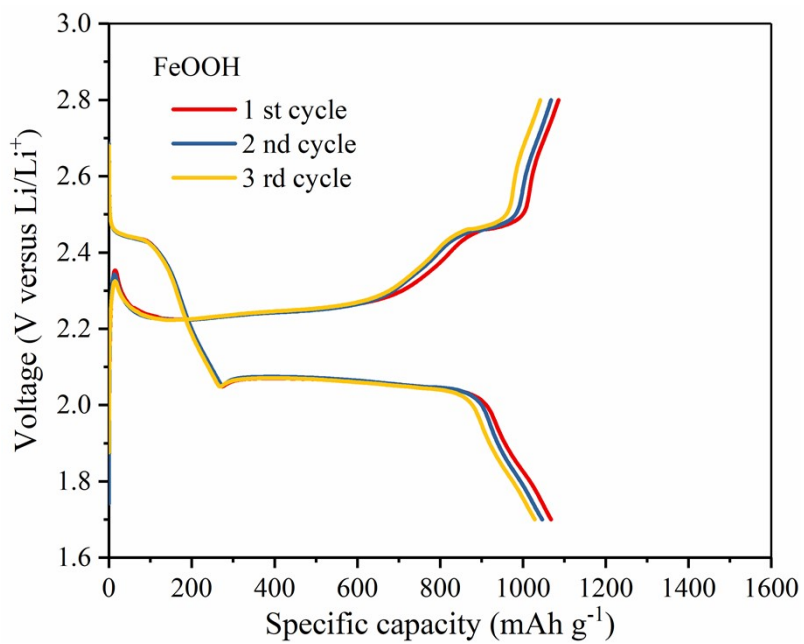


Fig. S9 Galvanostatic discharge/charge curves at 0.1 C of the batteries with FeOOH.

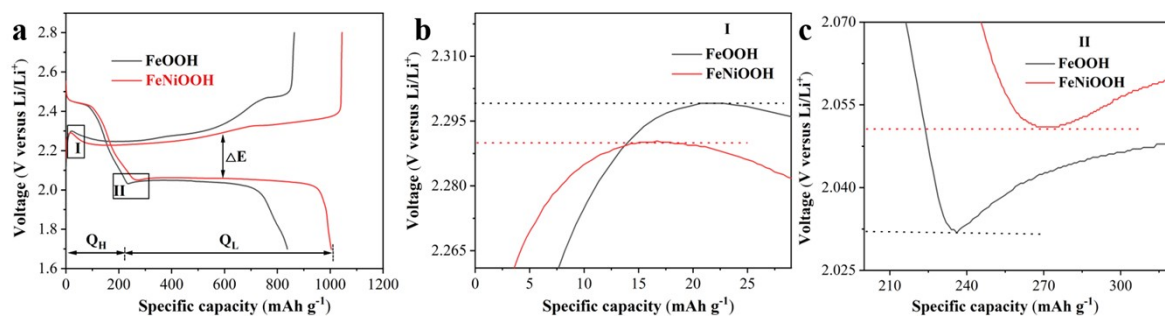


Fig. S10 Galvanostatic discharge/charge profiles of batteries with FeOOH and

FeNiOOH at a high sulfur loading of 5.1 mg cm<sup>-2</sup>.

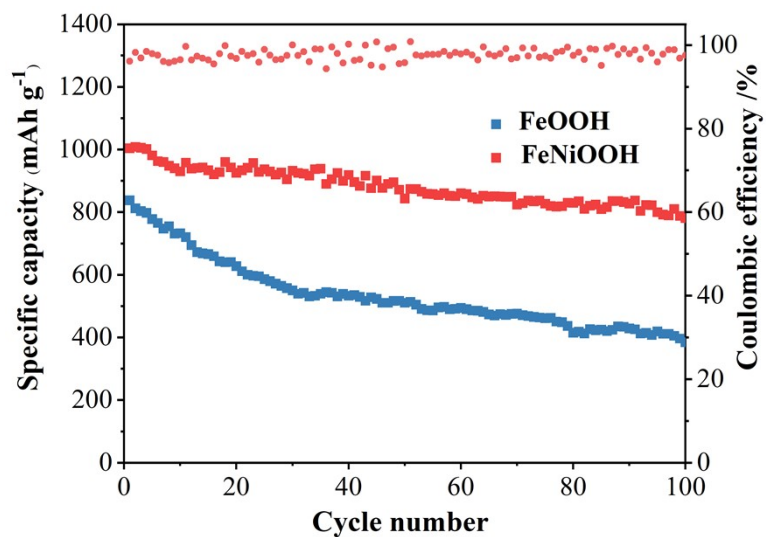


Fig. S11 Cycling performance of lithium sulfur batteries with a high sulfur loading of  $5.1 \text{ mg cm}^{-2}$  at  $0.1 \text{ C}$ .